

## Darcy-Stokes Equations with Finite Difference and Natural Boundary Element Coupling Method

Peng Weihong<sup>1</sup>, Cao Guohua<sup>2</sup>, Dongzhengzhu<sup>1</sup> and Li Shuncaï<sup>3</sup>

**Abstract:** Numerical method is applied to investigate the Darcy-Stokes equations, which is governing the steady incompressible Stokes flow past a circular cavity in a porous medium. The free fluid flow is modeled by the incompressible Stokes equations, and the flow in the porous medium is imposed by Darcy equations. Based on domain decomposition method with D-N alternating iteration algorithm, the coupling method of finite difference method and natural boundary element method is studied for the coupling Darcy-Stokes equations under a certain pressure difference. The numerical results indicate that the finite difference and natural boundary element coupling method is efficient and convenient for the Darcy-Stokes problem of the steady-state parallel flow with a void space.

**Keywords:** Darcy-Stokes, domain decomposition, D-N alternating iteration, coupling method.

### 1 Introduction

The combination of viscous incompressible flow and porous media flow occurs in many physical and engineering applications [Urquiza, Dri, Garon and Delfour(2008); Deng and Martinez(2005); Tan and Takashi (2005); Keh and Lu(2005)]. The problem is difficult to resolve because the underlying phenomena is diverse and the interactions between coupled flow systems are complex [Kanschat and Rivière(2010); Rui and Zhang(2009); Chen, Gunzburger and Wang(2010); Correa and Loula (2009)]. Correspondingly, it's tough to acquire the analytical solutions [Cai, Mu and Xu(2009); Boubendir and Tlupova(2009); Chidyagwai and Rivière(2009)]. The low Reynolds number flow over a porous spherical shell was analyzed [Jones(1973)]. In this model, Stokes equations were imposed within and without the spherical shell, and the Darcy's law was considered in the shell re-

---

<sup>1</sup> School of Mechanics and Civil Engineering, CUMT, Xuzhou, China

<sup>2</sup> School of Mechatronic Engineering, CUMT, Xuzhou, China

<sup>3</sup> School of Mechanical and Electrical Engineering, Xuzhou Normal University, Xuzhou, China

gion. The analytical expressions of velocities, pressures and resultant forces of the spherical shell are deduced in above three regions with the separation of variables technique. If the thickness of the spherical shell is infinitely thin, it can be treated as a membrane. Consequently, it was considered as the simple model for the infiltration of blood leukocytes [Zeng and Wu(1989)]. In this case, above three regions were simplified to two regions, and the transmembrane normal velocity depended on the pressure difference of the fluid within and without the spherical shell. On the interface of the porous medium and free flow, the normal velocity and the pressure were continuous. If the Permeability coefficient was small, the tangential velocity can also be regarded as continuity, and the non-slip condition is tenable. On the contrary, if the Permeability coefficient was large, the slip condition for the tangential velocity should be proposed.

On the other hand, the cavity often exists in an unbounded porous medium. The void space can change the flow field of groundwater seepage, and the Seepage velocity is difficult to calculate accurately. Thus, it is important to find a theory to study the flow field with a borehole in the porous medium. Fortunately, the viscous flows past a cavity in a porous medium were studied by some scholars. Two-dimensional viscous flow past a circular cavity in a porous medium was studied with Series method by Japanese scholar [Raja Sekhar and Sano(2001)], the calculation method of which was complex. In this paper, the coupling of the incompressible Stokes equations and Darcy equations are considered. The free fluid flow is modeled by the incompressible Stokes equations, and the flow in the porous medium is imposed by Darcy equations. Simultaneous, the model is coupled with the appropriate interface conditions. The coupling method of finite difference method and natural boundary element method [Yu(1993)] is applied to investigate the Darcy-Stokes equations, which is based on domain decomposition method with the Dirichlet-Neumann(D-N) alternating iteration algorithm.

## 2 Governing equations and boundary conditions

A two-dimensional coupling Darcy-Stokes problem is considered. A cavity exists in an unbounded homogeneous porous medium, and the cavity radius is  $R$ . The fluid flows along  $x$ -axis from infinity with velocity  $U_\infty$  under the pressure difference  $\Delta h$ . The flow far away from the void space is undisturbed, which can be considered as parallel flow. Suppose the entrance pressure is  $h_e$ , and the exit pressure is  $h_w$ . Thereby,  $h_e - h_w = \Delta h$ . The geometry model and boundary conditions are shown in Fig.1.

As to the steady-state parallel flow without void space, the pressure distribution is

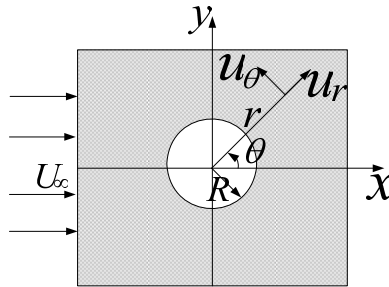


Figure 1: Void in porous media

linear along flow direction.

$$h(x) = h_e - (h_e - h_w) \frac{x}{L} \tag{1}$$

where  $h(x)$  is the pressure at arbitrary point of  $x$ -axis.

The Darcy' law is applied to represent non-inertial and incompressible flows in porous media with small porosity, where  $r > R$ . Thus, the pressure  $h$  is satisfied with the following equation.

$$-\frac{K}{\mu} \nabla^2 h = 0 \tag{2}$$

where  $K$  is the permeability coefficient,  $\mu$  is the dynamic viscosity. The Stokes equations is used for the void space, where  $r < R$ .

$$\begin{cases} \nabla \cdot \mathbf{u} = 0 \\ -\mu \Delta \mathbf{u} + \nabla p = 0 \end{cases} \tag{3}$$

On the interface of the circular void space and the porous medium, the velocities and the pressure are continuous, the transmission conditions of which are proposed as follows.

$$\begin{cases} u_r = v_r \\ u_\theta = v_\theta \\ p = h \end{cases} \tag{4}$$

where  $u_r, u_\theta, p$  represent the radial velocity, tangential velocity and pressure of the free flow in cavity;  $v_r, v_\theta, h$  are the radial velocity, tangential velocity and pressure of the flow in the porous medium.

### 3 Finite difference and natural boundary integral coupling method

#### 3.1 Dimensionless form of the problem

Apply the variables to dimensionless firstly.

$$(\bar{x}, \bar{r}) = \frac{(x, r)}{R}, \quad \bar{u} = \frac{u}{U_\infty}, \quad \bar{p} = p / (\mu \frac{U_\infty}{R}), \quad \bar{K} = K / R^2 \tag{5}$$

Correspondingly, the governing equations in porous medium can be expressed as follows.

$$\bar{\nabla}^2 \bar{h} = 0 \tag{6}$$

Similarly, the dimensionless form of Stokes flow in the void space can be obtained.

$$\begin{cases} \bar{\nabla} \cdot \bar{u} = 0 \\ -\Delta \bar{u} + \bar{\nabla} \bar{p} = 0 \end{cases} \tag{7}$$

For convenience, the superscript symbol will be dropped hereafter.

The flow far away from the void space is undisturbed, thus the finite circular region is divided from the unbounded porous medium. The cavity radius  $R = 1$ , the external diameter of porous medium  $R_1 = 3$ , the entrance pressure  $h_e = 10$ , the exit pressure  $h_w = 0$ , the specific geometry model and boundary conditions are given in Fig.2.

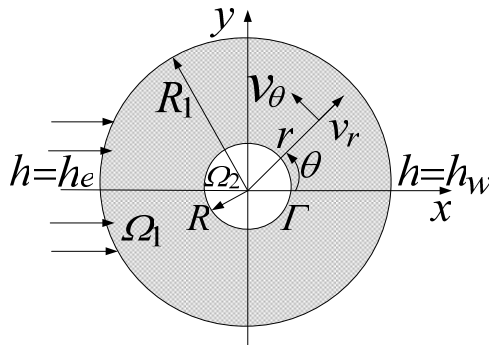


Figure 2: Geometric model and boundary conditions

### 3.2 Domain decomposition method

Divide the whole domain into two non-intersecting bounded subdomains  $\Omega_1$  and  $\Omega_2$ . The boundary of cavity is the artificial boundary  $\Gamma$ . The fan shaped grid is used to mesh  $\Omega_1$  in polar coordinates. Then, the finite difference method is applied to resolve the Darcy' law in domain  $\Omega_1$ . Thus, the pressure at arbitrary node can be attained. According to the relationship of velocity and pressure, the radial velocity and tangential velocity on the artificial boundary would be acquired. Afterwards, based on Newton-Cotes numerical integration formula, utilize the velocity value on artificial boundary and calculate in domain  $\Omega_2$  with natural boundary element method. Remarkably, the initial pressure value should be given before iterating, and the new value on the artificial boundary can be obtained with finite difference method in domain  $\Omega_1$ . Finally, the natural boundary element method is applied in domain  $\Omega_2$  and the new pressure value will be educed again. Iterate in turn, the results will be achieved with rational precision. The detailed alternating iteration algorithm is given as the following steps.

First, choose the initial value of pressure  $\lambda^0$  on the artificial boundary.

Second, apply the finite difference method to investigate the Darcy's equation based on the pressure boundary condition, and the pressure  $\lambda^i$  can be found. Then utilize the relationships between the pressure and velocities to calculate the velocities in domain  $\Omega_1$ . The corresponding problems are given as follows.

$$\begin{cases} \nabla^2 h = 0 & \text{in } \Omega_1 \\ h^i = u_0 & \text{on } \Gamma_1 \\ h^i = \lambda^i & \text{on } \Gamma' \end{cases}$$

Third, impose the natural boundary element method to calculate in domain  $\Omega_2$  according to the velocities on the artificial boundary  $\Gamma$ . The corresponding equations are given as follows.

$$\begin{cases} -\mu \Delta u + \nabla p = 0 & \text{in } \Omega_2 \\ u_r^i = -\frac{K}{\mu} \frac{\partial h^i}{\partial n} & \text{on } \Gamma' \\ u_\theta^i = -\frac{K}{\mu} \frac{1}{r} \frac{\partial h^i}{\partial \theta} & \text{on } \Gamma' \end{cases}$$

Accordingly, the pressure  $\lambda^{i+1}$  can be obtained.

Fourth, let  $\lambda^i = \lambda^{i+1}$ . Go to next step if the pressure on the boundary  $\Gamma$  is satisfied with the object. Otherwise, go to the second step;

Then, calculate the pressure and velocities.

### 3.3 Arithmetic design

#### 3.3.1 Application of finite difference method in domain $\Omega_1$

In order to get the pressure at arbitrary node in the porous medium, the partial differential equation for seepage flow  $\nabla^2 h = 0$  should be transformed into difference equation in polar coordinate system. The strategy for mesh grid allocation is to use a fan shaped grid with  $m$  nodes in the  $\theta$ -direction and  $n$  nodes in the  $r$ -direction. Each node is defined by the couple  $(i, j)$  in the circular ring domain, and  $i = 0, 1, \dots, m, j = 0, 1, \dots, n$ . Additionally, the radial step length is  $\Delta r$ , the tangential step length is  $\Delta \theta$ . According to the Taylor formula of two variables function, the terms equal to or greater than quintic term can be neglected when the step length  $\Delta r$  and  $\Delta \theta$  are small enough. Therefore, the difference equation can be acquired.

$$\begin{aligned} &\left(\frac{4r_0^2\Delta\theta^2}{\Delta r^2} + 4\right)h_0 - \left(\frac{2r_0^2\Delta\theta^2}{\Delta r^2} + \frac{r_0\Delta\theta^2}{\Delta r}\right)h_1 - 2h_2 \\ &- \left(\frac{2r_0^2\Delta\theta^2}{\Delta r^2} - \frac{r_0\Delta\theta^2}{\Delta r}\right)h_3 - 2h_4 = 0 \end{aligned} \tag{8}$$

where  $h = h(r, \theta)$ ;  $r_0 = R + r_{i,j} = R + j\Delta r$ . Let  $h_0 = h_{i,j}$ , the functions of  $h_1$  to  $h_4$  can be expressed by the nodes similarly. Thus, the difference equation(8) can be expressed as follows.

$$\begin{aligned} &\left(\frac{4(R + j\Delta r)^2\Delta\theta^2}{\Delta r^2} + 4\right)h_{i,j} - \left(\frac{2(R + j\Delta r)^2\Delta\theta^2}{\Delta r^2} + \frac{(R + j\Delta r)\Delta\theta^2}{\Delta r}\right) \\ &\times h_{i,j+1} - 2h_{i+1,j} - \left(\frac{2(R + j\Delta r)^2\Delta\theta^2}{\Delta r^2} - \frac{(R + j\Delta r)\Delta\theta^2}{\Delta r}\right)h_{i,j-1} - 2h_{i-1,j} = 0 \end{aligned} \tag{9}$$

Accordingly,  $h_{i,j}$  can be calculated.

$$\begin{aligned} h_{i,j} = &\frac{2(R + j\Delta r)^2\Delta\theta^2 + (R + j\Delta r)\Delta\theta^2\Delta r}{4(R + j\Delta r)^2\Delta\theta^2 + 4\Delta r^2}h_{i,j+1} \\ &+ \frac{2\Delta r^2}{4(R + j\Delta r)^2\Delta\theta^2 + 4\Delta r^2}h_{i+1,j} + \frac{2(R + j\Delta r)^2\Delta\theta^2 - (R + j\Delta r)\Delta\theta^2\Delta r}{4(R + j\Delta r)^2\Delta\theta^2 + 4\Delta r^2}h_{i,j-1} \\ &+ \frac{2\Delta r^2}{4(R + j\Delta r)^2\Delta\theta^2 + 4\Delta r^2}2h_{i-1,j} \end{aligned} \tag{10}$$

Conveniently, let  $m = 36$  and  $n = 20$ . Suppose the initial pressure on the artificial boundary is  $\lambda^0$ , then the boundary condition is  $h_{i,0} = \lambda^0, i = 0, 1, \dots, 36$ .

The pressure and velocities far away from the void space are undisturbed and satisfied with the characteristics of parallel flow, thus the pressure on the external boundary  $\Gamma_1$  can be obtained according to Eq.1.

$$h_{i,20} = h_e - (h_e - h_w) \frac{R_1 + R_1 \cos(i \cdot \Delta\theta)}{2R_1}, \quad i = 0, 1, \dots, 20 \quad (11)$$

Utilizing the inside and outside of the pressure boundary conditions, the pressure value in domain  $\Omega_1$  can be calculated. Then, based on the relationship between the pressure and velocities,

$$u_r = -\frac{K}{\mu} \frac{\partial h}{\partial y} \quad (12)$$

$$u_\theta = -\frac{K}{\mu} \frac{1}{r} \frac{\partial h}{\partial \theta} \quad (13)$$

Then the radial and tangential velocities can be attained preparing for the calculation of domain  $\Omega_2$ .

### 3.3.2 Application of natural boundary element method in domain $\Omega_2$

Based on the Fourier series method or the Green function method, the pressure boundary integral formula of Stokes equations can be deduced as equation with natural boundary element method [Peng, Dong, Cao and Zhao(2008)].

$$h(r, \theta) = -\frac{2\mu}{r} \left\{ \left[ \cos \theta \left( r \frac{\partial}{\partial r} P(r, \theta) \right) - \sin \theta \frac{\partial}{\partial \theta} P(r, \theta) \right] * u_r(R, \theta) \right. \\ \left. + \left[ \sin \theta \left( r \frac{\partial}{\partial r} P(r, \theta) \right) + \cos \theta \frac{\partial}{\partial \theta} P(r, \theta) \right] * u_\theta(R, \theta) \right\} + \frac{1}{2\pi} \int_0^{2\pi} h(R, \theta) d\theta \quad (14)$$

$$u_r(r, \theta) = \left\{ \cos \theta P(r, \theta) + \frac{R^2 - r^2}{2r^2} \left[ \cos \theta \left( r \frac{\partial}{\partial r} P(r, \theta) \right) - \sin \theta \frac{\partial}{\partial \theta} P(r, \theta) \right] \right. \\ \left. - \frac{R^2 - r^2}{2\pi R r} \right\} * u_r(R, \theta) + \left\{ \sin \theta P(r, \theta) + \frac{R^2 - r^2}{2r^2} \left[ \sin \theta \left( r \frac{\partial}{\partial r} P(r, \theta) \right) \right. \right. \\ \left. \left. + \cos \theta \frac{\partial}{\partial \theta} P(r, \theta) \right] \right\} * u_\theta(R, \theta) \quad (15)$$

$$u_\theta(r, \theta) = \left\{ -\sin \theta P(r, \theta) + \frac{R^2 - r^2}{2r^2} \left[ \sin \theta \left( r \frac{\partial}{\partial r} P(r, \theta) \right) \right. \right. \\ \left. \left. + \cos \theta \frac{\partial}{\partial \theta} P(r, \theta) \right] \right\} * u_r(R, \theta) + \left\{ \cos \theta P(r, \theta) \right. \\ \left. - \frac{R^2 - r^2}{2r^2} \left[ \cos \theta \left( r \frac{\partial}{\partial r} P(r, \theta) \right) - \sin \theta \frac{\partial}{\partial \theta} P(r, \theta) \right] + \frac{R^2 - r^2}{2\pi R r} \right\} * u_\theta(R, \theta) \quad (16)$$

where  $P(r, \theta) = \frac{R^2 - r^2}{2\pi[R^2 + r^2 - 2rR\cos\theta]}$ ,  $u_r(R, \theta)$  is the radial velocity on the artificial boundary,  $u_\theta(R, \theta)$  is the tangential velocity on the artificial boundary, and  $*$  is the convolution integral. Thus, the distribution in domain  $\Omega_2$  can be resolved with Eq.14.

As can be known from the facts mentioned above, the radial and tangential velocities on the artificial boundary  $\Gamma$  are calculated with finite difference method, which are discrete values. Therefore, Newton-Cotes numerical integration formula is used and the first term of integral formula(14) is analyzed as follows in detail.

As  $P(r, \theta) = \frac{R^2 - r^2}{2\pi[R^2 + r^2 - 2rR\cos\theta]}$ , the derivative with respect to two variables  $r$  and  $\theta$  can be obtained.

$$P_\theta(r, \theta) = \frac{\partial P(r, \theta)}{\partial \theta} = \frac{-R \cdot r(R^2 - r^2)}{\pi[R^2 + r^2 - 2rR\cos\theta]^2} \sin\theta \tag{17}$$

$$P_r(r, \theta) = \frac{\partial P(r, \theta)}{\partial r} = \frac{-r}{\pi[R^2 + r^2 - 2rR\cos\theta]} - \frac{1}{2} \frac{R^2 - r^2}{\pi[R^2 + r^2 - 2rR\cos\theta]^2} (2r - 2R\cos\theta) \tag{18}$$

Accordingly, the first term of integral equation(14) can be expressed as follows.

$$\begin{aligned} f(r, \theta) &= -\frac{2}{r} \cos\theta \left( r \frac{\partial}{\partial r} P(r, \theta) \right) * u_r(R, \theta) \\ &= -\frac{2\eta}{r} \int_0^{2\pi} r \cos(\theta - \theta') \left\{ \frac{-r}{\pi[R^2 + r^2 - 2rR\cos(\theta - \theta')]} \right. \\ &\quad \left. - \frac{1}{2} \frac{R^2 - r^2}{\pi[R^2 + r^2 - 2rR\cos(\theta - \theta')]^2} \right\} u_r(R, \theta') d\theta' \end{aligned} \tag{19}$$

Newton-Cotes numerical integration formula(19) will be applied to calculate the integral formula of Eq.18.

$$C = \frac{b-a}{90} [7f(x_0) + 32f(x_1) + 12f(x_2) + 32f(x_3) + 7f(x_4)] \tag{20}$$

where  $x_k = a + kh$  ( $k = 0, 1, 2, 3, 4$ ),  $[a, b]$  is the integral interval,  $h = \frac{b-a}{4}$ ,  $C$  is the integral result.

Use a fan shaped grid with 36 nodes in the  $\theta$  -direction and 10 nodes in the  $r$  -direction, and let  $n$  and  $N$  represent the step length in the  $\theta$  -direction and the  $r$  -direction respectively. Thus, the ranges of the step index  $i$  and  $j$  are  $i = 0, 1, \dots, 36$ ,



$j = 0, 1, \dots, 10$ . Eq.19 can be acquired by the sum of function values at five discrete points according to Newton- cotes formula(20). Five values  $0, \pi/2, \pi, 3\pi/2, 2\pi$  are chosen for the corresponding radian  $\theta$ . It is easy to known that the functions  $f(x_0)$  to  $f(x_4)$  of the Newton-cotes equation can be shown as follows.

$$\begin{aligned}
 f_{i,j}(0) &= \cos(i \cdot n - 0) \cdot (j \cdot N) \\
 &\times \left\{ \frac{-j \cdot N}{\pi [R^2 + (j \cdot N)^2 - 2R(j \cdot N) \cos(i \cdot n - 0)]} \right. \\
 &\left. - \frac{1}{2} \cdot \frac{(R^2 - j \cdot N)^2}{\pi [R^2 + (j \cdot N)^2 - 2R(j \cdot N) \cos(i \cdot n - 0)]^2} \right. \\
 &\left. \times [2j \cdot N - 2R \cos(i \cdot n - 0)] \right\} u_{r_{0,0}}
 \end{aligned} \tag{21}$$

$$\begin{aligned}
 f_{i,j}(1) &= \cos(i \cdot n - \pi/2) \cdot (j \cdot N) \\
 &\times \left\{ \frac{-j \cdot N}{\pi [R^2 + (j \cdot N)^2 - 2R(j \cdot N) \cos(i \cdot n - \pi/2)]} \right. \\
 &\left. - \frac{1}{2} \cdot \frac{(R^2 - j \cdot N)^2}{\pi [R^2 + (j \cdot N)^2 - 2R(j \cdot N) \cos(i \cdot n - \pi/2)]^2} \right. \\
 &\left. \times [2j \cdot N - 2R \cos(i \cdot n - \pi/2)] \right\} u_{r_{9,0}}
 \end{aligned} \tag{22}$$

$$\begin{aligned}
 f_{i,j}(2) &= \cos(i \cdot n - \pi) \cdot (j \cdot N) \\
 &\times \left\{ \frac{-j \cdot N}{\pi [R^2 + (j \cdot N)^2 - 2R(j \cdot N) \cos(i \cdot n - \pi)]} \right. \\
 &\left. - \frac{1}{2} \cdot \frac{(R^2 - j \cdot N)^2}{\pi [R^2 + (j \cdot N)^2 - 2R(j \cdot N) \cos(i \cdot n - \pi)]^2} \right. \\
 &\left. \times [2j \cdot N - 2R \cos(i \cdot n - \pi)] \right\} u_{r_{18,0}}
 \end{aligned} \tag{23}$$

$$\begin{aligned}
 f_{i,j}(3) &= \cos(i \cdot n - 3\pi/2) \cdot (j \cdot N) \\
 &\times \left\{ \frac{-j \cdot N}{\pi [R^2 + (j \cdot N)^2 - 2R(j \cdot N) \cos(i \cdot n - 3\pi/2)]} \right. \\
 &\left. - \frac{1}{2} \cdot \frac{(R^2 - j \cdot N)^2}{\pi [R^2 + (j \cdot N)^2 - 2R(j \cdot N) \cos(i \cdot n - 3\pi/2)]^2} \right. \\
 &\left. \times [2j \cdot N - 2R \cos(i \cdot n - 3\pi/2)] \right\} u_{r_{27,0}}
 \end{aligned} \tag{24}$$

$$\begin{aligned}
 f_{i,j}(4) &= \cos(i \cdot n - 2\pi) \cdot (j \cdot N) \\
 &\times \left\{ \frac{-j \cdot N}{\pi [R^2 + (j \cdot N)^2 - 2R(j \cdot N) \cos(i \cdot n - 2\pi)]} \right. \\
 &- \frac{1}{2} \cdot \frac{(R^2 - j \cdot N)^2}{\pi [R^2 + (j \cdot N)^2 - 2R(j \cdot N) \cos(i \cdot n - 2\pi)]^2} \\
 &\left. \times [2j \cdot N - 2R \cos(i \cdot n - 2\pi)] \right\} u_{r_{0,0}}
 \end{aligned} \tag{25}$$

Thereby, the integral formula (19) is updated.

$$\begin{aligned}
 f_{i,j} &= -2 \frac{2\pi - 0}{90} (7f_{i,j}(0) + 32f_{i,j}(1) \\
 &+ 12f_{i,j}(2) + 32f_{i,j}(3) + 7f_{i,j}(4))
 \end{aligned} \tag{26}$$

Similarly, the numerical integral of Eq.14 can be calculated, and the pressure distribution in domain  $\Omega_2$  is resolved. Then, assign the pressure on the artificial boundary  $\Gamma$  to the initial pressure value  $\lambda^0$ , and iterate in turn, the results will be resolved accurately. When iteration steps are over 70000, the convergence solutions can be obtained.

The velocity distribution in domain  $\Omega_2$  can be achieved directly by the relationship between the pressure and velocities after obtaining the pressure on the artificial boundary  $\Gamma$ , which needs no iterating in order to reduce the computational time. Then, the fitting functions of velocities on the artificial boundary  $\Gamma$  can be derived by the discrete values. Finally, the velocity distributions is obtained by the velocity boundary integral formula (15) and (16) in the circular domain  $\Omega_2$ .

#### 4 Results and Analysis

The velocity distributions in the porous medium and void space are studied as follows with different permeability coefficient.

##### 4.1 Permeability coefficient $K = 0.05$

The curve of horizontal velocities  $v_x$  along  $x$ -direction and  $y$ -direction are given in Fig.3 and Fig.4.

It is observed from Fig.3, the horizontal velocity is gradually decreasing with the increase of the distance from the center, and transferring to the porous medium relative smoothly. The highest horizontal velocity reaches at the center, and it is 2.5 times as much as the undisturbed. As can be seen from figure Fig.4, the horizontal velocity is rapidly diminishing with the raise of the distance from the center, and increasing slowly to the undisturbed velocity in order to fill the continuity condition on the artificial boundary.

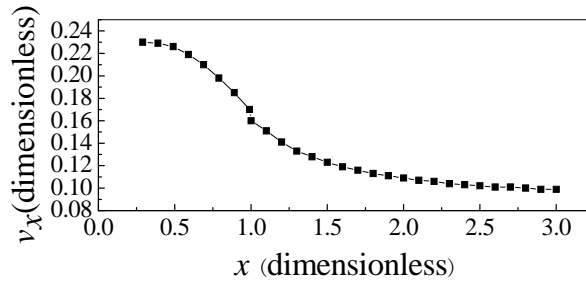


Figure 3: Relationship between  $v_x$  and  $x$ – direction

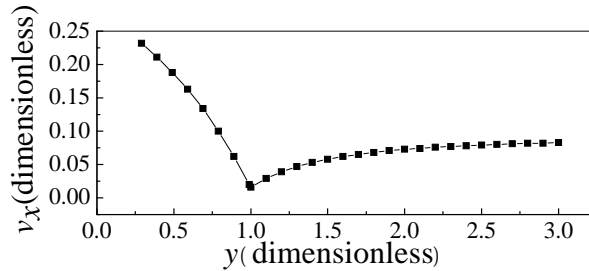


Figure 4: Relationship between  $v_x$  and  $y$ – direction

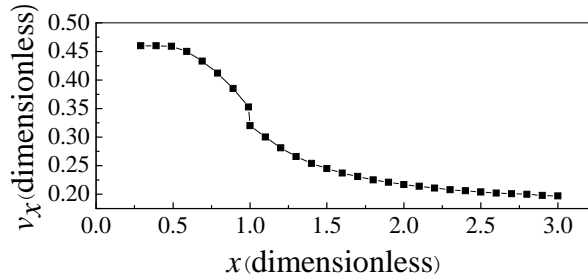
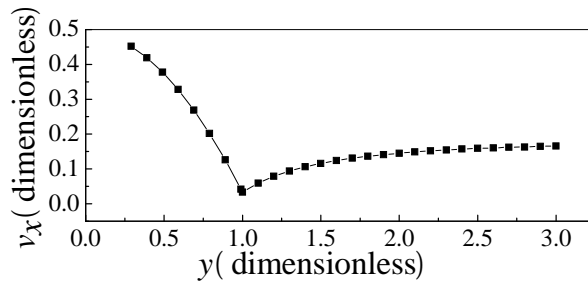
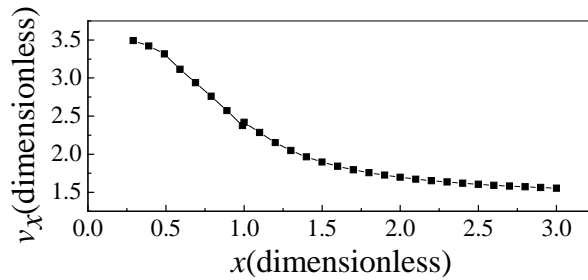
**4.2 Permeability coefficient  $K = 0.1$**

The curve of horizontal velocities  $v_x$  along  $x$ -direction and  $y$ -direction are shown in Fig.5 and Fig.6.

The curve of Fig.5 and Fig.6 are similar with the first case. By Comparison, the magnification of the highest value reduces appreciably, and it is 2.25 times as much as the undisturbed horizontal velocity.

**4.3 Permeability coefficient  $K = 0.8$**

The curve of horizontal velocities  $v_x$  along  $x$ -direction and  $y$ -direction are shown in Fig.7 and Fig.8. The curve of this case is similar with above two cases. Differently, the magnification of the highest value reduces more, and it is 2 times as much as the undisturbed horizontal velocity. The transmission from the porous medium to the free flow is more smoothing.

Figure 5: Relationship between  $v_x$  and  $x$ - directionFigure 6: Relationship between  $v_x$  and  $y$ - directionFigure 7: Relationship between  $v_x$  and  $x$ - direction

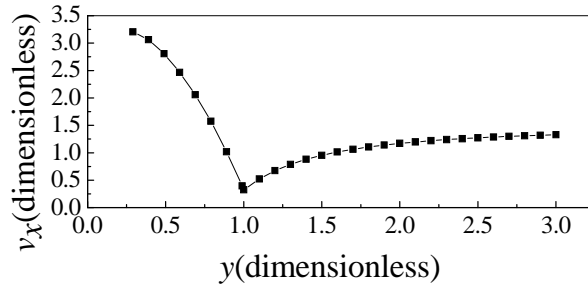


Figure 8: Relationship between  $v_x$  and  $y$ - direction

The velocity vector distribution can also be obtained by the finite difference and natural boundary element coupling method. The velocity vector distributions in the porous medium and the cavity are given in Fig.9 and Fig.10.

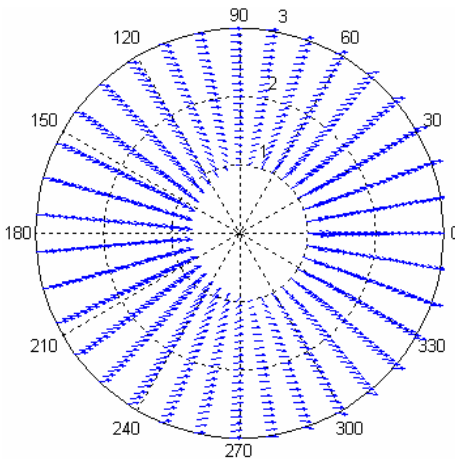


Figure 9: Velocity in the porous media

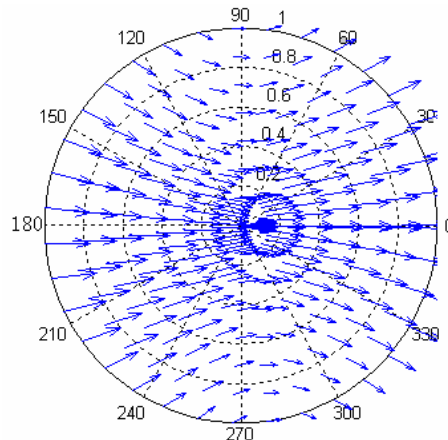


Figure 10: Velocity in the cavity

The results of above cases in this paper are according to reference [Raja Sekhar and Sano(2001)]. In order to validate the coupling method of natural boundary element method and finite difference method, the velocity vector distribution is analyzed as Fig.11 when the radius of the cavity  $R \rightarrow 0$ . It shows that the velocity vectors are parallel to  $x$  axis from the high pressure to the low pressure as reference [Kong(1999)].

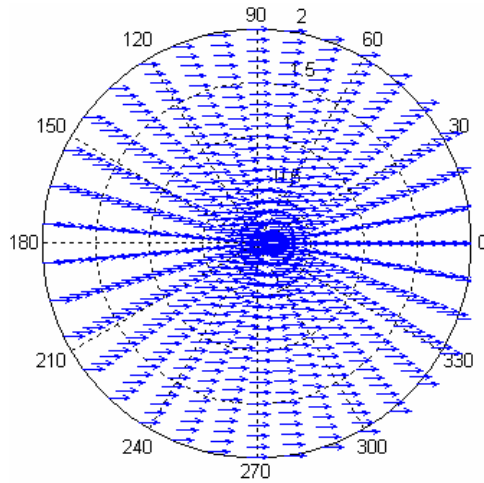


Figure 11: Velocity in the porous media without cavity

## 5 Conclusions

1. Based on domain decomposition method with the D-N alternating iteration algorithm, the coupling method of finite difference method and natural boundary element method is convenient and efficient to investigate the Darcy-Stokes equations.
2. As to the steady-state parallel flow with a void space, the velocity is increasing with the permeability coefficient under the same pressure difference.
3. The horizontal velocity is gradually decreasing with the increase of the distance from the center, and transferring to the porous medium relative smoothly on the artificial boundary in  $x$  direction.
4. The horizontal velocity is rapidly decreasing with the raise of the distance from the center, and increasing slowly to the undisturbed velocity in order to fill the continuity condition on the artificial boundary.

**Acknowledgement:** This research is sponsored by the “National Science Foundation for Young Scientists of China”(50909093); the “Youth Research Fund of China University of Mining and Technology” (2008A012); the “973 project” (2007-CB209400) and the “National Science Foundation of China” (50974107).

## References

- Boubendir, Y.; Tlupova S.** (2009): Stokes–Darcy boundary integral solutions using preconditioners. *Journal of Computational Physics*, Vol. 228, pp. 8627–8641.
- Cai, M.C.; Mu, M.; Xu J.C.** (2009): Preconditioning techniques for a mixed Stokes/Darcy model in porous media applications. *Journal of Computational and Applied Mathematics*, Vol. 233, pp. 346–355.
- Chen, N.; Gunzburger, M.; Wang, X. M.** (2010): Asymptotic analysis of the differences between the Stokes–Darcy system with different interface conditions and the Stokes–Brinkman system. *Journal of Mathematical Analysis and Applications* . Vol. 368, pp. 658–676.
- Chidyagwai, P.; Rivière, B.** (2009): On the solution of the coupled Navier–Stokes and Darcy equations. *Comput. Methods Appl. Mech. Engrg.*, Vol. 198, pp. 3806–3820.
- Correa, M.R.; Loula, A.F.D.** (2009): A unified mixed formulation naturally coupling Stokes and Darcy flows. *Comput. Methods Appl. Mech. Engrg.* Vol. 198, pp. 2710–2722.
- Deng, C.; Martinez, D.M.** (2005): Viscous flow in a channel partially filled with a porous medium and with wall suction. *Chemical Engineering Science*, vol. 60, no. 2, pp. 329–336.
- Jones, I.P.** (1973): Low Reynolds number flow over a porous spherical shell. *Camb. Phil. Soc.*, vol. 73, no. 1, pp. 231–238.
- Kanschat, G.; Rivière, B.** (2010): A strongly conservative finite element method for the coupling of Stokes and Darcy flow. *Journal of Computational Physics*, Vol. 229, pp. 5933–5943
- Keh, H.J.; Lu, Y.S** (2005). Creeping motions of a porous spherical shell in a concentric spherical cavity. *Journals of Fluids and Structures*, vol. 20, no. 5, pp. 735–747.
- Kong, X. Y.** (1999): *Advanced Mechanics of Fluids in Porous Media*. University of Science and Technology of China Press.
- Marin, Liviu** (2010): Stable Boundary and Internal Data Reconstruction in Two-Dimensional Anisotropic Heat Conduction Cauchy Problems Using Relaxation Procedures for an Iterative MFS Algorithm. *CMC: Computers, Materials & Continua*, vol. 17, no. 3, pp. 233–274.
- Peng, W. H.; Dong, Z.Z.; Cao, G.H.; Zhao, H. M.** (2008): Research on velocity solutions of Stokes flow in exterior circular region. *Journal of China University of Mining and Technology*, Vol. 37 No. 3, pp. 422–427.

**Raja Sekhar, G.P.; Sano, O.** (2001): Two-dimensional viscous flow past a slightly deformed circular cavity in a porous medium. *Fluid Dynamics Research*, vol. 28, no. 4, pp. 281-293.

**Rui, H.x.; Zhang, R.** (2009): A unified stabilized mixed finite element method for coupling Stokes and Darcy flows *Comput. Methods Appl. Mech. Engrg.* Vol. 198, pp. 2692–2699.

**Tan, W.C.; Takashi, M.** (2005): Stokes' first problem for a second grade fluid in a porous half-space with heated boundary. *International Journal of Non-linear Mechanics*, vol. 40, no. 4, pp. 515-522.

**Urquiza, J.M.; Dri, D.N'; Garon, A.; Delfour, M.C.** (2008): Coupling Stokes and Darcy equations. *Applied Numerical Mathematics*, vol. 58, pp. 525-538.

**Yu, D. H.** (1993): *Mathematics Theory of National Boundary Element Method.* Science Republic.

**Zeng, Y., Wu, W.Y.** (1989): A new analytical solution of Stokes equation. *Chinese Science Bulletin*, vol. 34, no. 20, pp. 1536-1539.